Formulation of polyphthalaldehyde microcapsules for immediate UV-light triggered release

Downloaded from: https://research.chalmers.se, 2025-12-04 08:24 UTC

Citation for the original published paper (version of record):

Eriksson, V., Andersson Trojer, M., Vavra, S. et al (2020). Formulation of polyphthalaldehyde microcapsules for immediate UV-light triggered release. Journal of Colloid and Interface Science, 579: 645-653. http://dx.doi.org/10.1016/j.jcis.2020.06.024

N.B. When citing this work, cite the original published paper.

research.chalmers.se offers the possibility of retrieving research publications produced at Chalmers University of Technology. It covers all kind of research output: articles, dissertations, conference papers, reports etc. since 2004. research.chalmers.se is administrated and maintained by Chalmers Library

(article starts on next page)

Journal of Colloid and Interface Science 579 (2020) 645–653

Contents lists available at ScienceDirect

Journal of Colloid and Interface Science

journal homepage: www.elsevier.com/locate/jcis

Formulation of polyphthalaldehyde microcapsules for immediate UV-light triggered release

Viktor Eriksson [a], Markus Andersson Trojer [b], Szilvia Vavra [a], Mats Hulander [a], Lars Nordstierna [a,*]

[a] Department of Chemistry and Chemical Engineering, Chalmers University of Technology, Göteborg, Sweden
[b] Department of Chemistry, Biomaterials and Textiles, Fiber Development, RISE IVF, Mölndal, Sweden

GRAPHICAL ABSTRACT

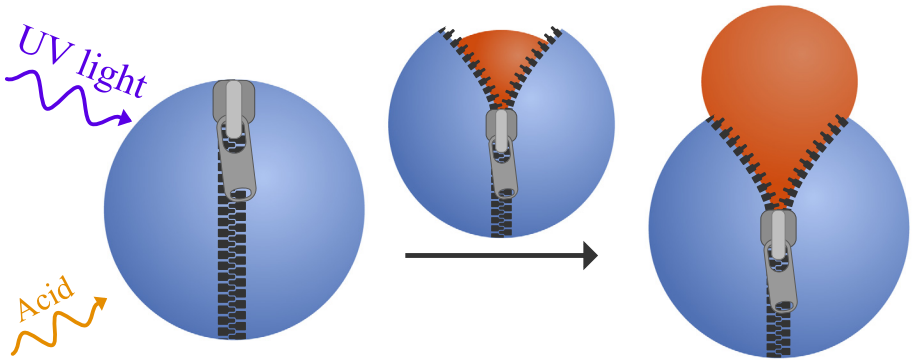

ARTICLE INFO

Article history:
Received 18 March 2020
Revised 5 June 2020
Accepted 6 June 2020
Available online 23 June 2020

Keywords:
Polyphthalaldehyde
Core–shell particle
Triggered release
Internal phase separation

ABSTRACT

Triggered release from responsive drug reservoirs activated by remote stimuli is desired in a range of fields. Critical bottlenecks are cost-efficient formulation avenues applicable for industrial scale-up, viable triggers and immediate release rather than continuous release upon activation. UV-sensitive microcapsules based on self-immolating polymers in combination with thin shells and morphological weak spots should allow for immediate triggered release. Polyphthalaldehyde-based microcapsules were prepared using several variations of the internal phase separation route. In addition, a fluorescence microscopy method was developed to study both the microcapsule morphology and the triggered release in-situ. The microcapsule formation was driven by the surface activity of the stabilizer, effectively lowering the high polymer-water interfacial tension, which is in sharp contrast to conventional encapsulation systems. Contrary to previous findings, a core–shell morphology was obtained via slow emulsion-to-suspension transformation. Rapid transformation captured intermediate inverted core–shell structures. The capsules were highly sensitive to both acid- and UV-mediated triggers, leading to an unzipping and rupturing of the shell that released the core content. Poly(methacrylic acid)-stabilized microcapsules displayed immediate UV-triggered release provided by their stimuli-sensitive blueberry morphology. Both capsules in aqueous and dry environment started to lose their core content after less than one minute of UV light exposure.

© 2020 The Author(s). Published by Elsevier Inc. This is an open access article under the CC BY license (http://creativecommons.org/licenses/by/4.0/).

* Corresponding author.
E-mail address: lars.nordstierna@chalmers.se (L. Nordstierna).

https://doi.org/10.1016/j.jcis.2020.06.024
0021-9797/© 2020 The Author(s). Published by Elsevier Inc.
This is an open access article under the CC BY license (http://creativecommons.org/licenses/by/4.0/).

1. Introduction

Encapsulation of actives into microcapsules is a widespread method for obtaining either sustained or triggered release of actives. A triggered release that is targeted and in particular sudden is of relevance for several applications, ranging from drug delivery to self-healing materials [1,2]. However, immediate release upon external stimuli is rarely reported in the literature. For microcapsules, triggered release usually denotes a continuous release during an interval ranging from several minutes to hours. For the considerable majority of microcapsule systems of core–shell structure, it is the shell that responds to an external stimulus. The release from the microcapsule can be triggered by a multitude of external stimuli, including pH, temperature and light irradiation among others [3–6]. The use of light as external stimulus has several advantages. It allows for the trigger to be remotely administered without the requirement of direct contact. In addition, the light stimulus that triggers the release can be wavelength-specific which allows for designing release systems with different triggerable events, each controlled by a precise wavelength.

For achieving light-triggered release from microcapsules, several approaches can be conceived. Nanoparticles embedded in the shell can act as catalysts for shell decomposition [4,7,8]. Polymers containing light-sensitive groups along the backbone can decompose without the requirement of nanoparticles [9,10]. One such polymer is polyphthalaldehyde (PPA), which is of particular interest since its light-triggered degradation is at the timescale of minutes. It has potential use in several applications such as photoresists, thermal scanning probe lithography and as a self-immolative polymer (SIP). As a SIP, advantages compared to other SIPs such as fast depolymerization kinetics and better control over polydispersity index can be seen [11].

Only a few very recent reports have investigated the formulation and triggered release from PPA microcapsules. DiLauro et al. [12] formulated microcapsules which were sensitive to fluoride, and Tang et al. [13,14] formulated acid-sensitive PPA microcapsules. In this paper, we have used PPA as a UV light-sensitive shell material for achieving immediate triggered release from a core–shell particle with a hydrophobic liquid core. The thermodynamic spreading conditions have been determined to further understand the encapsulation process and the different microcapsule morphologies obtained with different PPA systems. Being able to visualize the immediate release, that happens on the scale of minutes, is of high importance. Therefore, a microscopy methodology for studying the release from both particles in an aqueous suspension and dried onto a substrate is presented. This methodology made it possible to study changes in the capsule shell and the actual release of oil phase *in situ*, as compared to only monitoring macroscopic release of actives into a release bath.

2. Theory

The theoretical framework for microcapsule formation, using the internal phase separation method, is presented below. Based on the interfacial tensions between the core, shell and surrounding water phase, a morphology of the microcapsules can be predicted. Furthermore, theoretical background for determining the surface energy of a solid phase, such as the shell material, is presented.

2.1. Internal phase separation for microencapsulation

The formulation methodology employed is based on the seminal work by Loxley and Vincent [15]. This methodology has been used extensively, both for microcapsules and for loaded microspheres [16–18]. Torza and Mason had earlier developed a theory based on the spreading coefficients to predict the morphology in a system of three immiscible liquids [19]. This theory was later expanded by Loxley and Vincent to include a solid polymer shell [15] and by ourselves to encompass the all solid polymer core polymer shell particles [20].

The spreading coefficients are defined by the interfacial tensions as exemplified by the spreading coefficient for the polymer phase (S_p) in Equation (1). In a similar manner, the corresponding spreading coefficients for the oil (S_o) and water (S_w) can be expressed.

$$S_p = \gamma_{ow} - \left(\gamma_{po} + \gamma_{pw}\right) \tag{1}$$

Under the condition $\gamma_{ow} > \gamma_{pw}$, there can only be three sets of different combinations of the spreading coefficients, Equations (2–4). Without this condition, an additional morphology could be predicted where the oil phase spreads around the polymer phase, forming an inverted core–shell particle.

$$S_o < 0;\ S_w < 0;\ S_p > 0, \tag{2}$$

$$S_o < 0;\ S_w < 0;\ S_p < 0, \tag{3}$$

$$S_o < 0;\ S_w > 0;\ S_p < 0. \tag{4}$$

When fulfilling the conditions in Equation (2) a core–shell morphology is predicted. For the conditions in Equation (3) "acorn" particles are predicted and the conditions in Equation (4) produce separated droplets of oil and polymer. The thermodynamically predicted morphologies for the polymer shell and liquid oil core can be seen in Fig. 1. There are also several morphologies found in the literature for which there is no canonical thermodynamic explanation, also seen in Fig. 1. These are so called "blueberry" particles, multi-core particles [21] and "raspberry" particles [20]. Blueberry particles display an indentation on the microcapsule surface, however the shell is still completely enveloping the core. Raspberry particles display multiple acorn-like domains rather than just one.

2.2. Determination of surface energy

The establishment of the spreading conditions above necessitates knowledge of the surface free energy of the polymer. We have therefore for the first time determined the surface free energy of polyphthalaldehyde using the formalism established by van Oss and coworkers [22] which has provided reliable results in previous similar research [16,23]. For a given liquid or solid *i,* the surface tension γ_i^{TOT} can be divided into Lifshitz-van der Waals interactions (γ_i^{LW}) and polar acid-base interactions (γ_i^{AB}) according to Equation (5). By measuring contact angles θ on surface *i* with several test liquids, the surface energy γ_S^{TOT} can be determined according to Equations (5–7). The test liquids have known γ_i^{LW}, and γ_i^{AB} can be calculated from electron-acceptor (γ_i^+) and electron-donor (γ_i^-) interactions by Equation (6). The Young-Dupré equation, Equation (8), is then used to determine the solid–liquid interfacial energy γ_{SL}.

$$\gamma_i^{TOT} = \gamma_i^{LW} + \gamma_i^{AB} \tag{5}$$

$$\gamma_i^{AB} = 2\sqrt{\gamma_i^+ \gamma_i^-} \tag{6}$$

$$1 + \cos(\theta)\gamma_L^{TOT} = 2\left\{\left(\gamma_S^{LW}\gamma_L^{LW}\right)^{1/2} + \left(\gamma_S^+\gamma_L^-\right)^{1/2} + \left(\gamma_S^-\gamma_L^+\right)^{1/2}\right\} \tag{7}$$

$$\gamma_S^{TOT} = \gamma_{SL} + \gamma_L^{TOT}\cos(\theta) \tag{8}$$

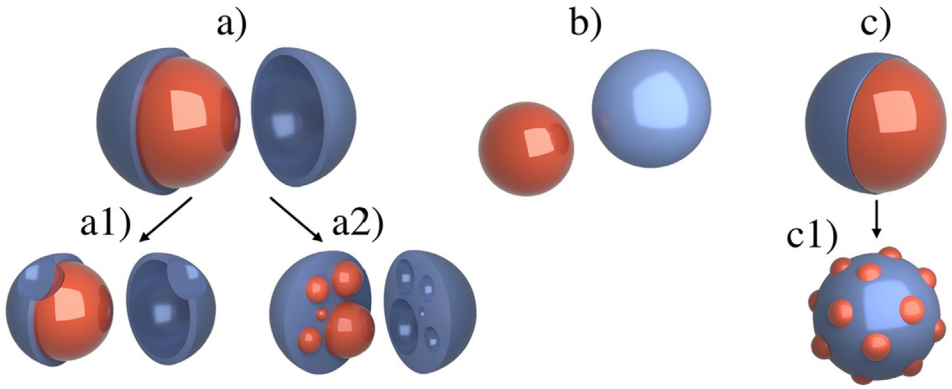

Fig. 1. Thermodynamically predicted morphologies for two-phase particles: a) cross-section of core–shell particle, b) core and shell material as separate particles or droplets, c) "acorn" particle. Several other morphologies have also been observed: a1) cross-section of "blueberry" particle, a2) cross-section of multi-core particle, c1) "raspberry" particle.

3. Experimental section

Polyphthalaldehyde (PPA, M_n 5–8 kDa, Sigma-Aldrich), dichloromethane (DCM, Sigma-Aldrich), diiodomethane (DIM, 99%, Sigma-Aldrich), glycerol (99%, Sigma-Aldrich), pyrene (≥99.0%, Sigma-Aldrich), formamide (99.5+%, Acros Organics), *n*-hexadecane (HD, 99%, Acros Organics), poly(vinyl alcohol) (PVA, 95% hydrolyzed, M_w 95 kDa, Acros Organics), poly(methacrylic acid) (PMAA, M_w 100 kDa, Polysciences Inc.) and acetone (≥99.8%, VWR Chemicals) were all used as received. The water used was of Milli-Q purity.

3.1. Microencapsulation

Microcapsules were formulated following the internal phase separation route, described by Loxley and Vincent [15] and previously modified by us [23]. A considerable scale-down in terms of working volume was however done. Hexadecane, a common model core substance, was chosen in order to allow for comparisons of the microcapsule morphology and the release behavior with the literature. In a real drug delivery system this would however have to be replaced with a different biocompatible oil such as a hydrophobic fatty acid ester or triglyceride. An oil phase consisting of 2.70 g DCM, 0.096–0.146 g PPA, 190 μl acetone and 0.098–0.151 g HD containing 2 wt% pyrene was prepared, giving shell-to-core ratios, m_s/m_c, ranging between 0.67 and 1.50. The oil phase was subsequently added slowly to 3 ml water phase containing 1 wt% of the stabilizer PVA or PMAA in a 5 ml round bottom flask with a side neck (Ace glass) that was immersed in a room-temperature water bath. This was carried out while stirring at 9 000 rpm using a Silent Crusher M equipped with homogenizing tool 6F (Heidolph Instruments, Germany). PVA and PMAA were chosen as stabilizers to investigate two different systems where the interfacial tensions differed. A 1 wt% solution of the stabilizers has previously been determined to provide sufficient stabilization of the suspension [15]. Emulsification was carried out for 80 min before diluting the emulsion with an additional 4.5 ml water phase. Finally, the diluted emulsion was left in a fume hood in an open glass vial under gentle magnetic stirring for at least 15 h for the volatile solvents to evaporate. No further purification was required for the microcapsule suspension after evaporation of the volatile solvents. An alternate evaporation was performed by rotary evaporating the volatile solvents at reduced pressure. This was done using an R-200 Rotavapor equipped with a B-490 heating bath kept at 25 °C (Büchi, Switzerland) and a MZ-2C diaphragm vacuum pump (Vacuubrand, Germany). By using rotary evaporation, the evaporation time was reduced to 30 min. PPA was protected from light by aluminum foil during all stages of the formulation to prevent any degradation.

3.2. Optical tensiometry

The surface tension, interfacial tension and contact angle of the liquids and substrates were determined using a Theta optical tensiometer (Attension, Finland) by fitting the drop shape with the Young-Laplace equation, Equation (9), where γ is the surface or interfacial tension, $\Delta\rho$ the density difference between the drop and the surrounding medium, g the gravitational constant, R_0 the radius at the drop apex and β the shape factor.

$$\gamma = \Delta\rho g R_0^2/\beta \tag{9}$$

For each combination at least three measurements were made. A summary of all combinations of liquids and substrates are presented in the Supporting Material.

3.2.1. Surface energy calculations

The surface energy of PPA was calculated using the formalism developed by van Oss and coworkers [22]. The Lifshitz contribution, as well as the polar acid and base contributions, was obtained from measurements of the contact angles of DIM, formamide, glycerol, hexadecane, and water on the substrate. PPA substrate samples were prepared on 22 × 22 mm glass slides by spin coating a 1 wt% solution of PPA in DCM using a Spin 150 spin coater (SPS-Europe, Netherlands). The spin coating was performed at 2 000 rpm for 60 s. The surface energy components were obtained using non-linear regression analysis in MatLab (Mathworks, USA). The details are presented in the Supporting Material.

3.3. Microscopy

The morphologies and sizes of microcapsules were analyzed using both light and fluorescence microscopy with an Axio Imager Z2m (Zeiss, Germany) equipped with an HBO-lamp and filter sets 38HE and 49 for fluorescence imaging. PPA was found to exhibit autofluorescence, and pyrene was added as a fluorophore to further elucidate the morphology of the microcapsules since differentiation between hexadecane and PPA is difficult based on only brightfield micrographs. Pyrene was chosen as it is highly hydrophobic, which made it distribute well in the hexadecane core. This is not the case for several other commonly used hydrophobic dyes, such as Disperse Red 13 and Sudan I, which tend to distribute well in the polymeric shell as well. Furthermore, the

excitation and emission wavelengths differed from those of PPA which allowed for differentiation using optical filters. Fluorescence micrographs obtained by using the two different fluorescence filters were combined with brightfield micrographs in post-processing, resulting in composite color-coded micrographs were hexadecane regions appeared in blue and PPA regions in purple.

3.3.1. Size distribution

The size distribution of microcapsules in a sample prepared by the solvent evaporation method is dependent on the initial size distribution of the emulsion prior to solvent evaporation. The emulsion droplet size has been found to follow a log-normal size distribution for a variety of systems [24,25]. It is therefore assumed that the size distribution of produced microcapsules also follows a log-normal size distribution, according to Equation (10), where M and S are the mean and standard deviation of the natural logarithm of the radius.

$$p(r) = \frac{1}{\sqrt{2\pi}Sr}\exp\left(-\frac{(\ln r - M)^2}{2S^2}\right) \qquad r > 0 \qquad (10)$$

The log-normal fitting was performed based on particle counting using the image-processing software ImageJ (National Institute of Health, USA). A total of five microscopy images from each sample were analyzed, or at least 600 particles, using an automated approach.

3.3.2. Analysis of dry capsules

For analyzing dry samples, an aliquot of the microcapsule suspension was diluted with eight parts Milli-Q water before adding a drop to a microscope glass slide. The glass slide was tilted to spread out the droplet before leaving it to dry completely. In dry state it was possible to monitor individual capsules before and after longer periods of exposure to UV light since the capsules stuck to the substrate.

3.3.3. Scanning electron microscope (SEM) analysis

The stock suspension of microcapsules was diluted 1:8 in MilliQ water and a ~ 10 μl droplet was left to dry in a low-pressure chamber (water suction) overnight at room temperature on 8x8 mm sized silicon wafer cuts. Immediately before viewing in SEM, the samples were sputtered with approximately 5 nm Au in a Quorum Q150R sputter. SEM was performed on a Zeiss Ultra 55 FEG scanning electron microscope using 3–5 kV acceleration voltage and channel mixing between SE2 and InLens detectors at ratios between 70 and 90 %. Images were acquired at tilt angles between 0 and 45°.

3.4. Triggered release

In this work, the external stimuli of UV light, heat, and acidity, respectively, were investigated as potential triggers as PPA is known to be sensitive to all three. However, the main focal point was on the UV light-triggered release which was investigated for both microcapsules in suspension and for dry microcapsules.

UV light triggered release of microcapsules was achieved using excitation light from the fluorescence microscope (bandpass-filtered mercury arc lamp with λ_{max} = 365 nm and an intensity of 1 W/cm^2) when studying release *in situ*. This made it possible to monitor single microcapsules as function of time and not just an average of several capsules before and after exposure. For longer exposure times of ten minutes, an Osram HBO 100/2 lamp operated at 90 W and with an intensity of 437 W/m^2 was used.

For acid-triggered release, the suspension was diluted with HCl to yield a high final concentration of 0.5 M, in order to give a rapid triggering of the release. When studying temperature as a trigger, the water suspension was heated to 90 °C and kept at this temperature for a total time period of up to one hour before evaluating the effects.

4. Results and discussion

In the following subsections, the detailed microcapsule characterization is presented. Capsule morphologies are described along with theoretical predictions using the thermodynamic spreading conditions as well as the kinetics during the internal phase separation process. Then, the investigation of the triggered release from the PPA-based microcapsules is presented. Two distinct sets of results are presented: those related to the formulation and those related to triggered release.

4.1. Formulation

The effect of three parameters during the formulation were investigated; the shell-to-core ratio, the nature of the stabilizer, and the evaporation rate. The effect of shell-to-core ratio was investigated for PVA-stabilized microcapsules. Furthermore, the effect of the stabilizer was determined by formulating microcapsules stabilized with either 1 wt% PVA or

1 wt% PMAA in the water phase. Finally, the evaporation rate of the volatile solvents was altered, including both fast rotary evaporation at reduced pressure and slow evaporation at ambient pressure. A fast evaporation has previously been proposed to produce core–shell particles of higher quality for PPA-based microcapsules [14]. Given the low water solubility of hexadecane (6 μg/L [26]) the theoretical encapsulation efficiency should be close to 100% directly after formulation. The stability of the microcapsules was limited to a few weeks under normal storage conditions (a water suspension under gentle magnetic stirring at ambient temperature), causing the capsules to break over time. It was possible to freeze the microcapsule suspension for storage over longer periods of time. After thawing, most of the microcapsules were found to be intact.

The size histograms of prepared microcapsules fitted with log-normal distribution functions are presented in Fig. 2. Similarities in size distributions between all the produced microcapsules were observed. The microcapsules were consequently only affected to a minor degree by altering the shell-to-core ratio. Furthermore, the emulsification that was performed by mechanical stirring is bound

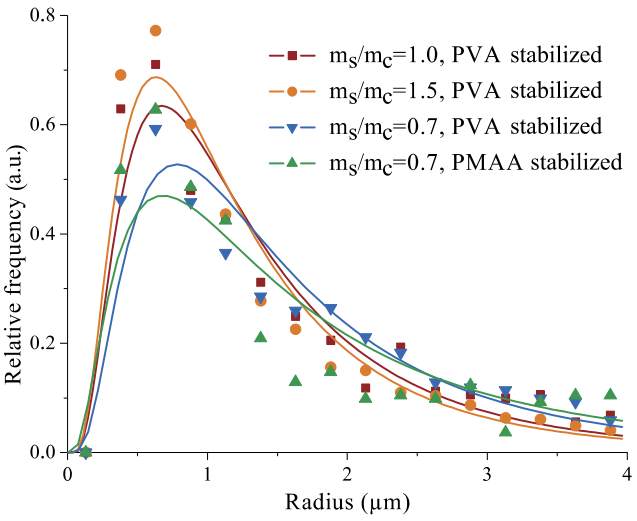

Fig. 2. Size distributions of prepared microcapsules with the experimentally determined data fitted to log-normal distribution functions.

to introduce variation in the size distributions from batch to batch. PMAA, being less surface active than PVA, produced microcapsules with a slightly larger average microcapsule radius and with a broadened distribution function.

4.1.1. Thermodynamic predictions and morphology observations

Calculated spreading coefficients for the two investigated microcapsule systems are presented in Table 1. See Supporting Material for full details. For the PVA-stabilized microcapsules, a core–shell morphology was predicted whereas the predicted morphology for PMAA-stabilized microcapsules was acorn particles. It should be noted that the theoretical calculations for PMAA are very close to core–shell and well within the experimental error. The observed morphologies for PVA-stabilized microcapsules were on the other hand found to be a fraction of core–shell particles and a fraction of acorn particles. Here the theoretically predicted morphology was close to the boundary between core–shell and acorn. For PMAA-stabilized microcapsules, so-called blueberry particles (see Section 2.1) were observed.

A high contact angle of above 90° for pure water on PPA was observed, suggesting that the polymer is highly hydrophobic. For a theoretical system without any dispersant in the water phase, the predicted morphology was consequently acorn particles. From a thermodynamical perspective, it was therefore the ability for PVA to effectively reduce the polymer-water interfacial tension that theoretically promoted the formation of core–shell particles. This is highly uncommon, since for liquid cores it is normally a maintained large γ_{ow}-value that drives the core–shell formation. More surface-active stabilizers are usually counteracting core–shell formation which does not appear to be the case for this particular system.

4.1.2. Effect of shell-to-core ratio

Contrary to the findings of Tang et al.[14] no dependency on m_s/m_c for producing core–shell or acorn particles could be found within the interval $0.67 < m_s/m_c < 1.50$. Instead, fractions of both core–shell and acorn particles were produced across the investigated m_s/m_c range. Fig. 3 shows an optical microscopy image where the insets are composite images of two fluorescence images with different filter sets. Regions in blue represent the hexadecane oil phase whereas purple regions represent the PPA shell. The greater purple fluorescence intensity in the shell of the microcapsule in the top inset, that also was more shifted towards red as compared to the core indicated that this was a core–shell morphology. Since the blue fluorescence from the oil phase was seen alone in the bottom inset, this showed that the oil was not encapsulated. Rather, it had formed an acorn particle with two hemispheres of hexadecane and PPA respectively. The thermodynamic spreading conditions were found to be on the boundary between core–shell and acorn. By having a slow evaporation of the volatile solvent, it allowed for obtaining a system in which minor interfacial tension fluctuations resulted in capsules of both core–shell and acorn morphology. When altering the m_s/m_c ratio, the thermodynamic spreading coefficients still remain constant which would not alter the microcapsule morphology. Although the formulation methods

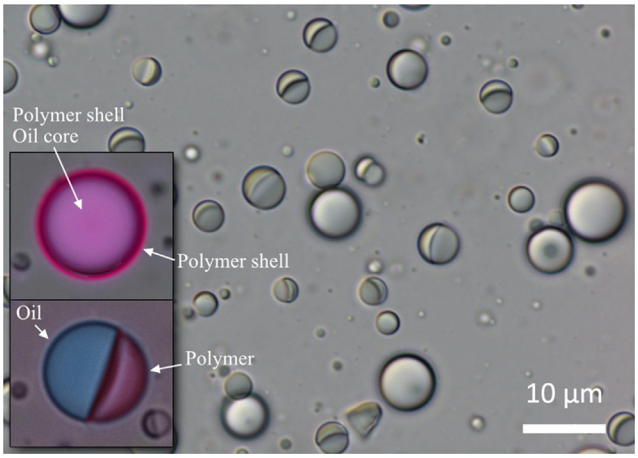

Fig. 3. Optical microscopy images of capsules stabilized with PVA (m_s/m_c = 0.67). Both core–shell particles and acorn particles could be observed. Insets show magnifications of composite images illustrating the morphology of the two microcapsule types: core–shell (top) and acorn (bottom). Hexadecane is seen in blue and PPA in purple. (For interpretation of the references to color in this figure legend, the reader is referred to the web version of this article.)

here differed slightly from those of Tang et al. [14], both methods were based on internal phase separation by solvent evaporation. Hence, the thermodynamics should be the same for both studies. Given that Tang et al. did not present the thermodynamic spreading conditions, it is possible that their morphology results originated from non-thermodynamic reasons.

4.1.3. Effect of stabilizer in water phase

The morphology of PPA microcapsules was strongly dependent on the dispersant used. PVA-stabilized capsules obtained a morphology distribution where one fraction was of core–shell structure and the other fraction, approximately similar in size, was of acorn structure. For PMAA-stabilized capsules, on the other hand, only blueberry particles were present as compared to the predicted acorn particles. Fig. 4 shows the difference in morphology between PVA and PMAA stabilized microcapsules. From the SEM micrograph, in the inset of Fig. 4 b, the surface indentation of a dried blueberry particle is clearly seen.

4.1.4. Effect of evaporation rate

By altering the evaporation rate, it was possible to determine how the kinetics of the spreading and solidification process affected the microcapsule morphology. Fig. 5 illustrates the effect of increasing the evaporation rate of the volatile solvent by using a rotary evaporator rather than evaporating at ambient pressure. Corresponding microcapsule systems formulated with a slow evaporation are presented in Fig. 4.

A slightly cratered core–shell structure was obtained for the PVA-stabilized microcapsules in Fig. 5a. The increased evaporation rate did not give the polymer enough time for relaxation during the coacervation process. Consequently, a smooth surface was not obtained but rather a cratered shell surface. This is in agreement

Table 1
Interfacial tensions and calculated spreading coefficients for the investigated systems. Indices o and p are the oil and polymer phases respectively, and w is the water phase as either pure water or a water phase containing 1 wt% of either PVA or PMAA. All units are in mN/m.

Emulsifier	γ_{ow}	γ_{op}	γ_{pw}	S_p	S_w	S_o	Morphology	
							Predicted	Observed
None	53.5	14.4	43.3	−4.2	−82.3	−24.7	Acorn	–
PVA	21.2	14.4	4.2	2.6	−11.0	−31.5	Core-shell	Acorn, core–shell
PMAA	33.4	14.4	19.4	−0.4	−38.4	−28.5	Acorn	Blueberry

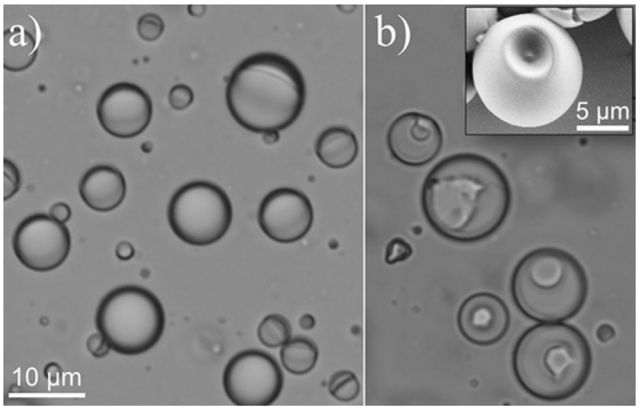

Fig. 4. Optical microscopy image illustrating the difference in microcapsule morphology when using (a) 1 wt% PVA or (b) 1 wt% PMAA as dispersant in the water phase. The scale bar is valid for both sub-figures. The inset in b) shows a SEM micrograph of a dried blueberry particle. Both microcapsule types were formulated with m_s/m_c = 0.67.

with what we have seen previously [16]. See inset in Fig. 5a for composite fluorescence image magnifications of a core–shell microcapsule (left) and an inverted core–shell microcapsule (right) where hexadecane is surrounding PPA.

PMAA-stabilized microcapsules similarly displayed cratered structures. This was seen to a much larger extent, giving a wrinkled appearance to the capsule shells. Equivalent to the microcapsules obtained via slow evaporation, blueberry particles were observed. Furthermore, polymeric spheres were seen inside the microcapsules. Insets in Fig. 5b show magnifications of a blueberry particle (left) and a blueberry particle with a polymer sphere inside it (right).

4.1.5. A summary of the driving forces for core–shell formation

Several insights were reached when studying the effects of shell-to-core ratio, stabilizer in the water phase and the evaporation rate. The shell-to-core ratio did not have any effect on the observed final morphologies of the microcapsules. However, the stabilizer had a profound effect on the morphological outcome via its influence on the γ_{pw} interfacial tension. It is plausible – yet speculative – that this influence also affects the rate of spreading and would therefore account for the observed blueberry morphology for the PMAA-stabilized microcapsules.

From studying the effect of evaporation rate, it was concluded that the polymer phase separated in the emulsion droplet before the core oil and that it did not have enough time to spread at the interface between water and emulsion droplet, which would be thermodynamically favored at equilibrium. Instead, only a small amount of polymer phase separated at this interface whereas the rest phase separated as solid polymeric spheres inside the core–shell structure. Thus, the kinetically favored morphology was an inverted core–shell particle whereas the thermodynamically favored morphology was a core–shell or acorn particle. The wrinkled core–shell particles displayed a decreased stability, most likely due to a thinner and coarser shell as a result of the polymer sphere formation inside the core–shell structure.

4.2. Triggered release

The triggered release from the microcapsules was investigated as a function of external stimuli mediated by UV light, heat, and acid, respectively. UV irradiation-triggered release from microcapsules was investigated *in situ* both for microcapsules in water suspension and for microcapsules dried onto a glass substrate. The degradation of PPA was further characterized by infrared spectroscopy. IR spectra before and after 10 min of UV light exposure are presented in the Supporting Material. After UV exposure the microfilm for IR analysis changed appearance from solid to viscous liquid. This is also presented in the Supporting Material. When adding HCl to the suspension, capsule shells could be seen to crack which exposed the interior oil phase. Heat-triggered release was also investigated. However, the effect was significantly weaker as compared to both UV light and HCl, and the results were inconclusive. See Supporting Material for data regarding acid and temperature triggered release.

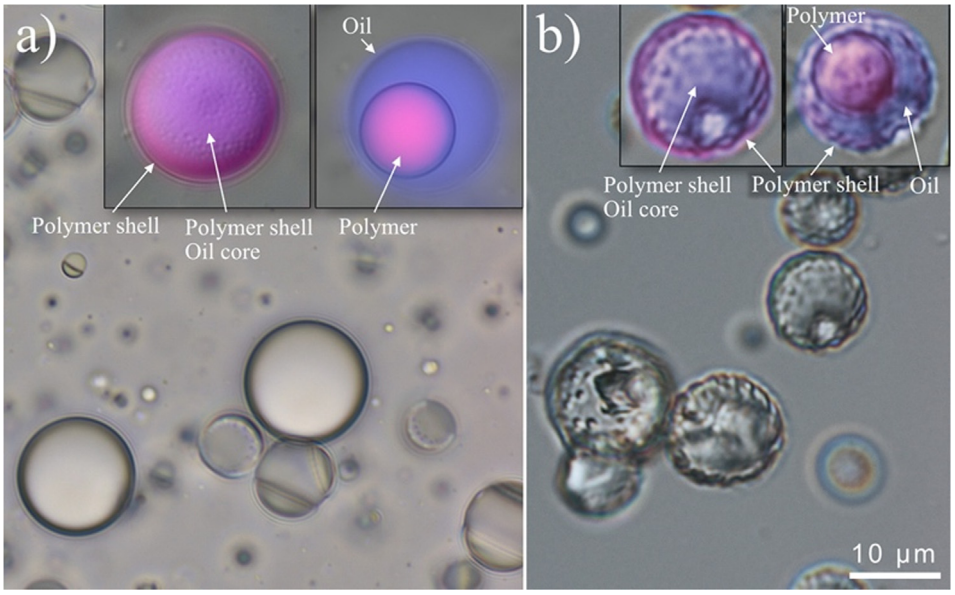

Fig. 5. Optical microscopy image illustrating the difference in microcapsule morphology of (a) PVA-stabilized and (b) PMAA-stabilized microcapsules when a fast evaporation of the volatile solvents was performed. The insets illustrate fluorescence-colored images representing the different observed microcapsule morphologies. Through fluorescence microscopy, polymer (purple) and oil (blue) regions could be identified. Both microcapsule types were formulated with m_s/m_c = 0.67. (For interpretation of the references to color in this figure legend, the reader is referred to the web version of this article.)

4.2.1. Capsules in suspension

Fig. 6 illustrates the triggered release from PMAA-stabilized microcapsules with m_s/m_c = 0.67. Due to the rapid changes in the microcapsules, capturing one brightfield and two fluorescence micrographs as in Fig. 3 for each time interval was not possible. Consequently, only one fluorescence micrograph was captured where both hexadecane and PPA is seen in blue. Pyrene present in the hexadecane showed a greater fluorescence intensity as compared to that from the PPA. A protruding oil phase was seen from the blueberry cavity in the shell surface after only one minute of exposure to light from the fluorescence microscope. After 5 min the entire oil phase had emerged from the ruptured microcapsule. The region of rupture for the microcapsules and the protruding oil phase has been marked by arrows in the three sub-figures. We hypothesize that the shell becomes thinner in the indentation area of the shell during the formulation. The indentation thus became the weakest point of the microcapsule and this was consequently the area of rupture. From a triggered release standpoint, this was highly beneficial as this made the capsules increasingly triggerable. Combined with the fact that all capsules in fact obtained this morphology, and not a fraction of acorn morphology, this was a superior system compared to PVA-stabilized microcapsules.

The blueberry core–shell morphology as well as the susceptibility of the blueberry indentation for deformation could be confirmed using SEM imaging. In Fig. 7, some of the PMAA-stabilized capsules were seen to break due to the evacuation during imaging, revealing the single core interior, which is a commonly observed phenomenon for single core–shell particles [23]. Moreover, many of the capsules that broke were seen to break in the indentation on the surface. This was further evidence that this indentation in fact was a weak spot of the microcapsule that could promote the behavior seen in Fig. 6.

For microcapsules formulated with PVA as a stabilizer, no immediate triggered release in suspension could be observed *in situ* when there was a slow evaporation of the volatile solvents during formulation, see Fig. 8. The fraction of core–shell particles did, however, obtain a dimpled surface after UV light exposure for a longer period of 10 min. As the irradiation was continued and monitored *in situ*, the surface became more and more dimpled over time. In addition to the surface-dimpled microcapsules, free oil droplets in the form of smooth spheres were seen. These originated from capsules that had broken prior to UV light exposure, during formulation or storage. It is possible that the blueberry morphology was key for immediate release and that the smallest shell thickness for the PVA-stabilized microcapsules was too thick to cause a rupture during the experimental conditions.

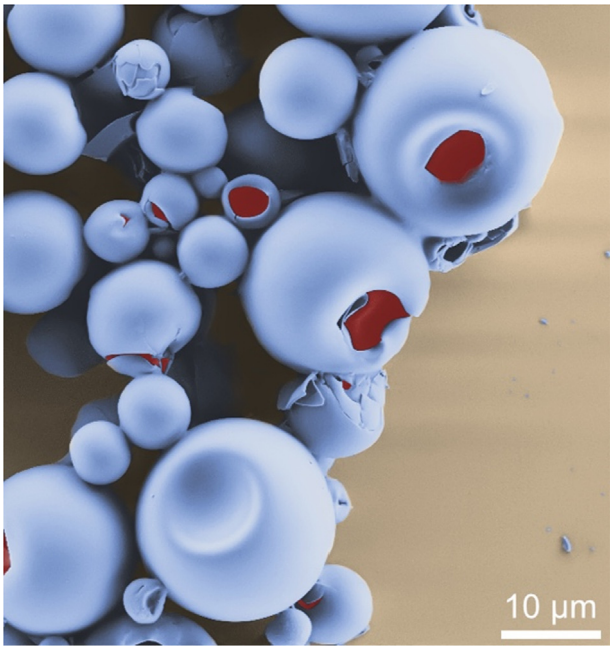

Fig. 7. Colored SEM micrograph of dried PMAA-stabilized microcapsules. Some of the blue microcapsules broke due to the drying or the vacuum during the imaging. These holes in the microcapsules are shown in red. Original micrograph is provided in Supporting Material. (For interpretation of the references to color in this figure legend, the reader is referred to the web version of this article.)

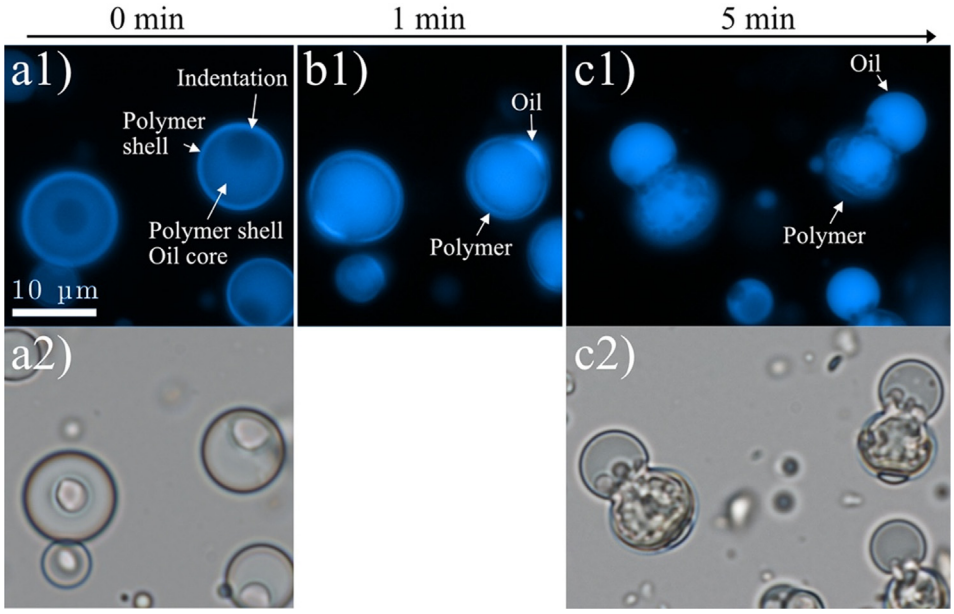

Fig. 6. Fluorescence and brightfield microscopy images of PMAA-stabilized microcapsules (m_s/m_c = 0.67) after a) 0 min., b) 1 min., and c) 5 min. of exposure to a filtered HBO lamp (λ_{max} = 365 nm) *in situ*. Both PPA and hexadecane is seen in blue. Brightfield images of the microcapsules in a1) and c1) can be seen in a2) and c2) respectively. Arrows in each subfigure a1)-c1) mark the region where the oil phase was protruding. The scale bar is valid for all sub-figures. (For interpretation of the references to color in this figure legend, the reader is referred to the web version of this article.)

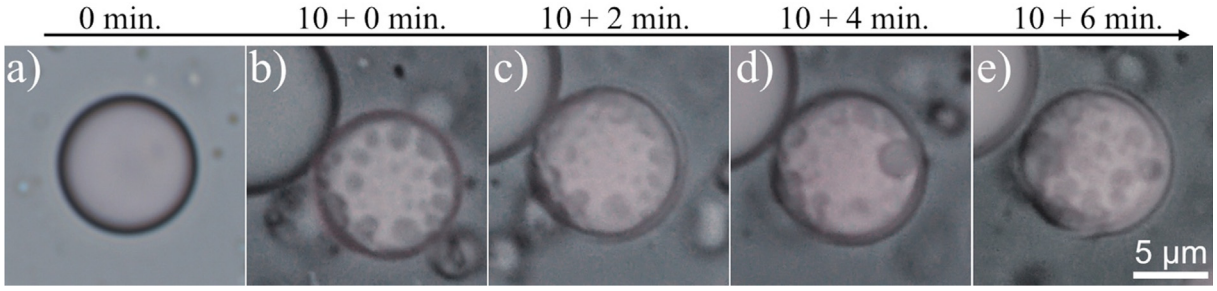

Fig. 8. PVA-stabilized microcapsules (m_s/m_c = 0.67) a) before exposure. Sub-figures b)-e) were subjected to 10 min of UV irradiation from an unfiltered HBO lamp, followed by b) 0 min., c) 2 min., d) 4 min., and e) 6 min of irradiation from a filtered HBO lamp (λ_{max} = 365 nm) and studied *in situ*. The scale bar is valid for all sub-figures.

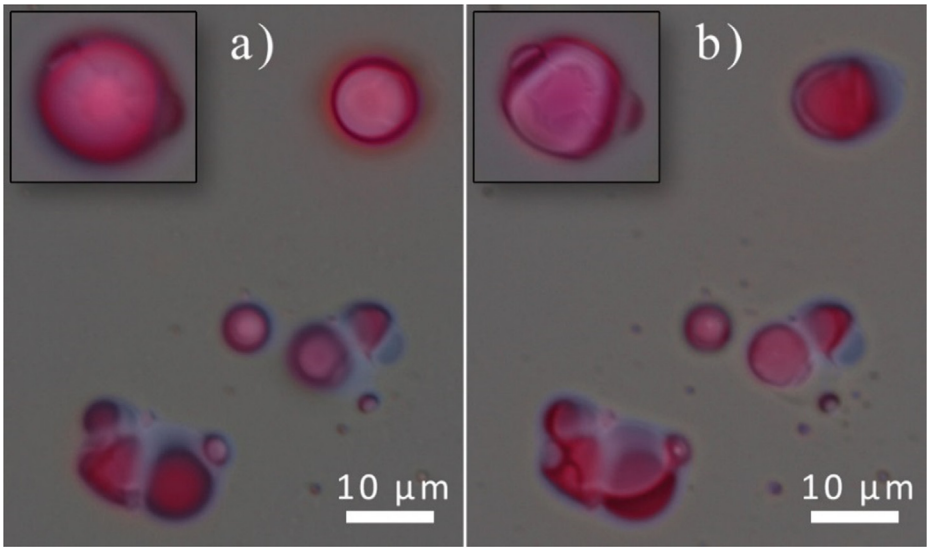

Fig. 9. Dried PVA-stabilized PPA microcapsules (m_s/m_c = 0.67) a) before and b) after less than one minute of irradiation from a filtered HBO lamp (λ_{max} = 365 nm). The insets illustrate a magnification of a microcapsule before and after irradiation.

When formulating PVA-stabilized microcapsules with fast rotary evaporation of the volatile solvent, triggered release of the core oil could be observed within seconds of exposure to UV light. Here, ruptures similar to those in Fig. 6 were observed, presented in the Supporting Material. During a fast evaporation process there was not enough time for the polymer to relax into its most energetically favored configuration. Instead, a porous shell was observed in which the polymer chains were at strain. This would reduce the mechanical stability of the microcapsules which in turn made triggered release possible.

4.2.2. Dry capsules and UV exposure

PVA-stabilized microcapsules were also dried and subsequently exposed to UV light. Prior to exposure to UV light, the microcapsules were found as intact particles on the surface. It should therefore be possible to store the microcapsules as a dry powder. After less than one minute of UV light irradiation, capsules could be seen to collapse. See Fig. 9 for a composite microscopy image comparing the same region of the sample before and after irradiation. Blue regions indicate the oil phase whereas the purple regions indicate the shell polymer. Small volumes of oil were seen to leak out from the microcapsules as a result of the irradiation.

5. Conclusions

Polyphthalaldehyde (PPA) microcapsules from which immediate release could be UV-triggered were formulated. Using a UV-responsive system enabled a remote stimulus to trigger the release instead of a physical change in the system, such as altering the pH. The blueberry morphology obtained using poly(methacrylic acid) (PMAA) as the dispersant was especially suited for triggered release. For this morphology, the inherent indentation provided an area from which the triggered release could proceed. Furthermore, the fact that all observed microcapsules obtained the blueberry morphology – as compared to only a fraction of the PVA-stabilized microparticles being of core–shell morphology – was beneficial. Tang et al. [13,14] rigorously investigated the formation of and quantified the triggered release from PPA microcapsules. Contradictory to Tang's findings, we have shown that it was not possible to kinetically trap core–shell morphologies by rapid solvent evaporation following the internal separation route. Rather, inverted core–shell particles were formed with an increased solvent evaporation rate while core–shell microcapsules were formed with a slower evaporation rate. We also showed that there was no difference in the obtained morphology in the interval 0.7–1.5 for the weight ratio of PPA shell material to hexadecane core oil.

What in fact was driving the core–shell formation was the ability of the dispersant to lower the shell-water interfacial tension, which is a unique characteristic of this particular material system that has not been previously reported. For more conventional core–shell systems, Loxley and Vincent [15] as well as our previous studies [20] have found a high core-water interfacial tension and less frequently a low core–shell interfacial tension to be the main driving forces for producing core–shell microcapsules.

The possibility to achieve immediate triggered release – both from microcapsules in a suspension and dried onto a substrate - is useful in a wide range of applications. To further enhance the microcapsule sensitivity towards UV light, photo acid generators could be incorporated into the shell. Upon UV light exposure, the photo acid generators would induce an acid-catalyzed depolymerization of the shell, enabling even faster shell unzipping.

Declaration of Competing Interest

The authors declare that they have no known competing financial interests or personal relationships that could have appeared to influence the work reported in this paper.

Acknowledgements

The Swedish Research Council FORMAS (2018 – 02284) and Vinnova (2017-04693 and 2019-04332) are acknowledged for funding.

Appendix A. Supplementary data

Supplementary data to this article can be found online at https://doi.org/10.1016/j.jcis.2020.06.024.

References

[1] A.P.R. Johnston, G.K. Such, F. Caruso, Triggering Release of Encapsulated Cargo, Angew. Chem. Int. Ed. 49 (15) (2010) 2664–2666.
[2] M.R. Kessler, N.R. Sottos, S.R. White, Self-healing structural composite materials, Compos. A Appl. Sci. Manuf. 34 (8) (2003) 743–753.
[3] A.P. Esser-Kahn, S.A. Odom, N.R. Sottos, S.R. White, J.S. Moore, Triggered release from polymer capsules, Macromolecules 44 (14) (2011) 5539–5553.
[4] K. Sato, K. Yoshida, S. Takahashi, J.-I. Anzai, pH-and sugar-sensitive layer-by-layer films and microcapsules for drug delivery, Adv. Drug Deliv. Rev. 63 (9) (2011) 809–821.
[5] K.Z. Chen, ShuxueFabrication of ultraviolet-responsive microcapsules via Pickering emulsion polymerization using modified nano-silica/nano-titania as Pickering agents, RSC Adv. 5 (18) (2015) 13850–13856.
[6] C.-H. Choi, J.-H. Jung, D.-W. Kim, Y.-M. Chung, C.-S. Lee, Novel one-pot route to monodisperse thermosensitive hollow microcapsules in a microfluidic system, Lab Chip 8 (9) (2008) 1544–1551.
[7] K. Katagiri, K. Koumoto, S. Iseya, M. Sakai, A. Matsuda, F. Caruso, Tunable UV-Responsive Organic−Inorganic Hybrid Capsules, Chem. Mater. 21 (2) (2009) 195–197.
[8] B. Radt, T.A. Smith, F. Caruso, Optically Addressable Nanostructured Capsules, Adv. Mater. 16 (23–24) (2004) 2184–2189.
[9] T. Dispinar, C.A.L. Colard, F.E. Du Prez, Polyurea microcapsules with a photocleavable shell: UV-triggered release, Polym. Chem. 4 (3) (2013) 763–772.
[10] N. Fomina, C. McFearin, M. Sermsakdi, O. Edigin, A. Almutairi, UV and Near-IR Triggered Release from Polymeric Nanoparticles, J. Am. Chem. Soc. 132 (28) (2010) 9540–9542.
[11] F. Wang, C.E. Diesendruck, Polyphthalaldehyde: Synthesis, Derivatives, and Applications, Macromol. Rapid Commun. 39 (2) (2018) 1700519.
[12] A.M. DiLauro, A. Abbaspourrad, D.A. Weitz, S.T. Phillips, Stimuli-Responsive Core-Shell Microcapsules with Tunable Rates of Release by Using a Depolymerizable Poly(phthalaldehyde) Membrane, Macromolecules 46 (9) (2013) 3309–3313.
[13] S. Tang, L. Tang, X. Lu, H. Liu, J.S. Moore, Programmable Payload Release from Transient Polymer Microcapsules Triggered by a Specific Ion Coactivation Effect, J. Am. Chem. Soc. 140 (1) (2018) 94–97.
[14] S. Tang, M. Yourdkhani, C.M. Possanza Casey, N.R. Sottos, S.R. White, J.S. Moore, Low-Ceiling-Temperature Polymer Microcapsules with Hydrophobic Payloads via Rapid Emulsion-Solvent Evaporation, ACS Appl. Mater. Interfaces 9 (23) (2017) 20115–20123.
[15] A. Loxley, B. Vincent, Preparation of poly (methylmethacrylate) microcapsules with liquid cores, J. Colloid Interface Sci. 208 (1) (1998) 49–62.
[16] J. Bergek, M. Andersson Trojer, A. Mok, L. Nordstierna, Controlled release of microencapsulated 2-n-octyl-4-isothiazolin-3-one from coatings: Effect of microscopic and macroscopic pores, Colloids Surf., A 458 (2014) 155–167.
[17] J. Bergek, M. Andersson Trojer, H. Uhr, L. Nordstierna, Controlled release of a microencapsulated arduous semi-hydrophobic active from coatings: Superhydrophilic polyelectrolyte shells as globally rate-determining barriers, J. Control. Release 225 (2016) 31–39.
[18] M.A. Trojer, H. Andersson, Y. Li, J. Borg, K. Holmberg, M. Nydén, L. Nordstierna, Charged microcapsules for controlled release of hydrophobic actives, Part III: the effect of polyelectrolyte brush- and multilayers on sustained release, Physical Chemistry Chemical Physics 15 (17) (2013) 6456–6466.
[19] S. Torza, S.G. Mason, Three-phase interactions in shear and electrical fields, J. Colloid Interface Sci. 33 (1) (1970) 67–83.
[20] M. Andersson Trojer, A. Ananievskaia, A.A. Gabul-Zada, L. Nordstierna, H. Blanck, Polymer Core-Polymer Shell Particle Formation Enabled by Ultralow Interfacial Tension Via Internal Phase Separation: Morphology Prediction Using the Van Oss Formalism, Colloid and Interface Science, Communications 25 (2018) 36–40.
[21] T. Trongsatitkul, B.M. Budhlall, Multicore-Shell PNIPAm-co-PEGMa Microcapsules for Cell Encapsulation, Langmuir 27 (22) (2011) 13468–13480.
[22] C.J. Van Oss, R.J. Good, M.K. Chaudhury, Additive and nonadditive surface tension components and the interpretation of contact angles, Langmuir 4 (4) (1988) 884–891.
[23] M.A. Trojer, Y. Li, C. Abrahamsson, A. Mohamed, J. Eastoe, K. Holmberg, M.J.S.M. Nydén, Charged microcapsules for controlled release of hydrophobic actives. Part I: encapsulation methodology and interfacial properties, 9(5) (2013) 1468-1477.
[24] E.S. Rajagopal, Statistical theory of parcticle size distributions in emulsions and suspensions, Kolloid-Zeitschrift 162 (2) (1959) 85–92.
[25] K.J. Packer, C. Rees, Pulsed NMR studies of restricted diffusion. I. Droplet size distributions in emulsions, J. Colloid Interface Sci. 40 (2) (1972) 206–218.
[26] F. Franks, Solute-Water Interactions and the Solubility Behaviour of Long-chain Paraffin Hydrocarbons, Nature 210 (5031) (1966) 87–88.